J|A|C|S
ARTICLES
Published on Web 01/11/2007

FePt@CoS_2 Yolk−Shell Nanocrystals as a Potent Agent to Kill HeLa Cells

Jinhao Gao,[†] Gaolin Liang,[‡] Bei Zhang,[§] Yi Kuang,[#] Xixiang Zhang,[§] and Bing Xu*[,†,‡,#]

Contribution from the Department of Chemistry, Center for Cancer Research, Department of Physics, and Bioengineering Program, The Hong Kong University of Science and Technology, Clear Water Bay, Hong Kong, China

Received November 3, 2006; E-mail: chbingxu@ust.hk

Abstract: We report the evaluation of cytotoxicity of a new type of engineered nanomaterials, FePt@CoS_2 yolk−shell nanocrystals, synthesized by the mechanism of the Kirkendall effect when FePt nanoparticles serve as the seeds. The cytotoxicity of FePt@CoS_2 yolk−shell nanocrystals, evaluated by MTT assay, shows a much lower IC_{50} (35.5 ± 4.7 ng of Pt/mL for HeLa cell) than that of cisplatin (230 ng of Pt/mL). In the control experiment, cysteine-modified FePt nanoparticles exhibit IC_{50} at 12.0 ± 0.9 μg of Pt/mL. Transmission electron microscopy confirms the cellular uptake of FePt@CoS_2 nanocrystals, and the magnetic properties analysis (SQUID) proves the release of FePt nanoparticles from the yolk−shell nanostructures after cellular uptake. These results are significant because almost none of the platinum-based complexes produced for clinical trials in the past 3 decades have shown higher activity than that of the parent drug, cisplatin. The exceptionally high toxicity of FePt@CoS_2 yolk−shell nanocrystals (about 7 times higher than that of cisplatin in terms of Pt) may lead to a new design of an anticancer nanomedicine.

Introduction

This paper reports the potent cytotoxicity of FePt@CoS_2 yolk−shell nanocrystals toward cancer cells (e.g., HeLa cells) and bacteria (e.g., *Bacillus* spp.). Recently, the rapid development of nanoscale science and technology[1] has led to increased research efforts into the applications of nanomaterials in biology and medicine.[2] Cobalt chalcogenide hollow nanocrystals, first reported by Yin and co-workers,[3] represent a novel class of engineered nanomaterials that may find broad applications in nano-optics system, catalysis, and drug delivery. Cobalt chalcogenide hollow nanocrystals form easily by the mechanism of the Kirkendall effect.[3,4] During the formation of the hollow structure, cobalt atoms diffuse toward the outer layer to generate the void. In this process, many pores also form in the cobalt chalcogenide shell. As demonstrated by Yin et al., small molecules such as hydrogen, ethylene, and ethane are able to enter into the interior of the shell or diffuse out of the shell freely through the pores.[3] This result implies that water molecules should cross the porous shell because of the polar surface of Co_xS_y, which would further allow ions to pass through the shell. Therefore, the yolk or the core inside the shell can interact with biological systems via the mediation of water. The successful synthesis of Pt@CoO yolk−shell nanostructures[3] and the well-known anticancer drug based on the binding of platinum ions to DNA[5] (e.g., cisplatin) encouraged us to evaluate the cytotoxicity of yolk−shell nanostructures containing platinum as a potential candidate for the development of an anticancer nanomedicine. To monitor the dissolution of the yolk, we chose

[†] Department of Chemistry.
[‡] Center for Cancer Research.
[§] Department of Physics.
[#] Bioengineering Program.

(1) Murray, C. B.; Kagan, C. R.; Bawendi, M. G. *Science* **1995**, *270*, 1335. Peng, X. G.; Manna, L.; Yang, W. D.; Wickham, J.; Scher, E.; Kadavanich, A.; Alivisatos, A. P. *Nature* **2000**, *404*, 59. Sun, Y. G.; Xia, Y. N. *Science* **2002**, *298*, 2176. Whitesides, G. M.; Mathias, J. P.; Seto, C. T. *Science* **1991**, *254*, 1312. Xia, Y. N.; Yang, P. D.; Sun, Y. G.; Wu, Y. Y.; Mayers, B.; Gates, B.; Yin, Y. D.; Kim, F.; Yan, Y. Q. *Adv. Mater.* **2003**, *15*, 353. El-Sayed, M. A. *Acc. Chem. Res.* **2001**, *34*, 257. Hyeon, T.; Lee, S. S.; Park, J.; Chung, Y.; Bin Na, H. *J. Am. Chem. Soc.* **2001**, *123*, 12798.

(2) Bruchez, M.; Moronne, M.; Gin, P.; Weiss, S.; Alivisatos, A. P. *Science* **1998**, *281*, 2013. Cui, Y.; Wei, Q. Q.; Park, H. K.; Lieber, C. M. *Science* **2001**, *293*, 1289. Lewin, M.; Carlesso, N.; Tung, C. H.; Tang, X. W.; Cory, D.; Scadden, D. T.; Weissleder, R. *Nat. Biotechnol.* **2000**, *18*, 410. Cao, Y. W. C.; Jin, R. C.; Mirkin, C. A. *Science* **2002**, *297*, 1536. Gu, H. W.; Ho, P. L.; Tsang, K. W. T.; Wang, L.; Xu, B. *J. Am. Chem. Soc.* **2003**, *125*, 15702. Xu, C. J.; Xu, K. M.; Gu, H. W.; Zhong, X. F.; Guo, Z. H.; Zheng, R. K.; Zhang, X. X.; Xu, B. *J. Am. Chem. Soc.* **2004**, *126*, 3392. Xu, C. J.; Xu, K. M.; Gu, H. W.; Zheng, R. K.; Liu, H.; Zhang, X. X.; Guo, Z. H.; Xu, B. *J. Am. Chem. Soc.* **2004**, *126*, 9938. Reynolds, R. A.; Mirkin, C. A.; Letsinger, R. L. *J. Am. Chem. Soc.* **2000**, *122*, 3795. Rosi, N. L.; Thaxton, C. S.; Mirkin, C. A. *Angew. Chem., Int. Ed.* **2004**, *43*, 5500. Jain, P. K.; Qian, W.; El-Sayed, M. A. *J. Am. Chem. Soc.* **2006** *128*, 2426. So, M. K.; Xu, C. J.; Loening, A. M.; Gambhir, S. S.; Rao, J. H. *Nat. Biotechnol.* **2006**, *24*, 339. Huh, Y. M.; Jun, Y. W.; Song, H. T.; Kim, S.; Choi, J. S.; Lee, J. H.; Yoon, S.; Kim, K. S.; Shin, J. S.; Suh, J. S.; Cheon, J. *J. Am. Chem. Soc.* **2005**, *127*, 12387. Zhang, Y.; So, M. K.; Loening, A. M.; Yao, H. Q.; Gambhir, S. S.; Rao, J. H. *Angew. Chem., Int. Ed.* **2006**, *45*, 4936. Zhang, Y.; So, M. K.; Rao, J. H. *Nano Lett.* **2006**, *6*, 1988. Lee, I. S.; Lee, N.; Park, J.; Kim, B. H.; Yi, Y. W.; Kim, T.; Kim, T. K.; Lee, I. H.; Paik, S. R.; Hyeon, T. *J. Am. Chem. Soc.* **2006**, *128*, 10658.

(3) Yin, Y. D.; Rioux, R. M.; Erdonmez, C. K.; Hughes, S.; Somorjai, G. A.; Alivisatos, A. P. *Science* **2004**, *304*, 711.

(4) Zhang, L. Z.; Yu, J. C.; Zheng, Z.; Leung, C. W. *Chem. Commun.* **2005**, *21*, 2683. Tu, K. N.; Gosele, U. *Appl. Phys. Lett.* **2005**, *86*, 093111. Wang, Y. L.; Cai, L.; Xia, Y. N. *Adv. Mater.* **2005**, *17*, 473. Gao, J. H.; Zhang, B.; Zhang, X. X.; Xu, B. *Angew. Chem., Int. Ed.* **2006**, *45*, 1220. Fan, H. J.; Knez, M.; Scholz, R.; Nielsch, K.; Pippel, E.; Hesse, D.; Zacharias, M.; Gosele, U. *Nat. Mater.* **2006**, *5*, 627.

(5) *The Pharmacological Basis of Therapeutics*, 9th ed.; Hardman, J. G., Limbird, L. E., Molinoff, P. B., Ruddon, R. W., Eds.; McGraw-Hill: New York, 1995.

10.1021/ja067785e CCC: $37.00

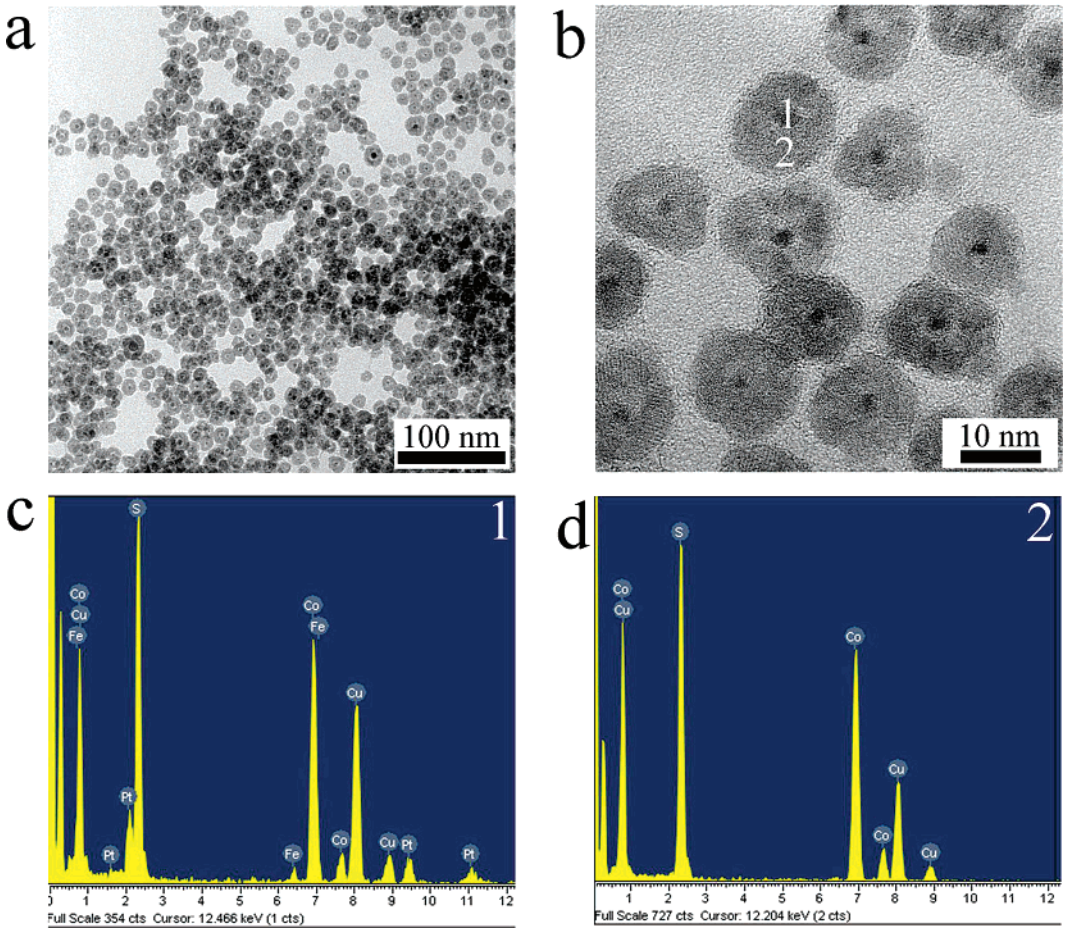

Figure 1. Characterization of FePt@CoS_2 yolk−shell nanocrystals. (a) TEM and (b) HRTEM images of FePt@CoS_2 yolk−shell nanocrystals. EDX analysis of the core part (c) and the shell part (d), corresponding to regions 1 and 2 in panel b, respectively.

FePt nanoparticles as the seeds to produce FePt@CoS_2 yolk−shell nanocrystals because the superparamagnetism of FePt nanoparticles[6] should allow one to monitor the dissolution of the yolk using a sensitive instrument such as a superconducting quantum interference device (SQUID).

After making the FePt@CoS_2 yolk−shell nanocrystals, we used an MTT assay of HeLa cells to evaluate the cytotoxicity of the FePt@CoS_2 nanocrystals. The MTT analysis indicated that the IC_{50} (the concentration of drug required to inhibit cell growth by 50% compared to the control) of the FePt@CoS_2 nanocrystals is about 35.5 ± 4.7 ng of Pt/mL, which is much lower than that of cisplatin (230 ng of Pt/mL).[7] These results are significant because almost none of the platinum-based complexes produced for clinical trials in the past 3 decades has shown higher activity than that of the parent drug, cisplatin.[7] On the other hand, few nanomaterials have been studied for anticancer therapy. The exceptionally high anticancer activity of FePt@CoS_2 yolk−shell nanocrystals (about 7 times higher than that of cisplatin in terms of Pt) may lead to a new class of candidates for use as anticancer drugs.

Results and Discussion

After obtaining FePt nanoparticles by the thermal decomposition of $Pt(acac)_2$ and $Fe(CO)_5$ according to the procedure reported by Sun and co-workers,[6] without any separation and purification, we directly injected the 1,2-dichlorobenzene solution of $Co_2(CO)_8$ into the refluxing solution containing oleic acid, FePt nanoparticles, and trioctylphosphine oxide (TOPO) surfactant to give the FePt@Co core−shell intermediates (Supporting Information, Figure S1). After another 30 min, injection of a solution of sulfur in 1,2-dichlorobenzene into the hot mixture resulted in a black dispersion of FePt@CoS_2 yolk−shell nanocrystals within a few seconds. As shown in the transmission electron microscopy (TEM) image (Figure 1a), the FePt@CoS_2 yolk−shell nanocrystals are similar to Pt@CoO yolk−shell nanocrystals,[3] indicating that the same Kirkendall effect process on cobalt layers affords the FePt@CoS_2 yolk−shell nanocrystals. The high-resolution TEM (HRTEM) image (Figure 1b) suggests that both the FePt parts and the CoS_2 parts are crystalline. Energy-dispersive X-ray spectrometric (EDX) analysis (Figure 1c,d) further confirms that the core mainly consists of Fe and Pt and the shell mainly consists of Co and S. Moreover, X-ray photoelectron spectroscopic (XPS) measurement of FePt@CoS_2 yolk−shell nanocrystals (Figure S2), performed immediately after the growth of the CoS_2 shell, gives dominant signals of Co and S in the spectrum, with very weak peaks of Fe and Pt or even the absence of them. The XPS measurement on the surface of the yolk−shell nanocrystals thus supports the mechanism of the growth of the shell because the XPS signal strongly depends upon the distance of the constituent atoms from the surface of the nanocrystals. X-ray fluorescence

(6) Sun, S. H.; Murray, C. B.; Weller, D.; Folks, L.; Moser, A. *Science* **2000**, *287*, 1989.
(7) Giovagnini, L.; Ronconi, L.; Aldinucci, D.; Lorenzon, D.; Sitran, S.; Fregona, D. *J. Med. Chem.* **2005**, *48*, 1588.

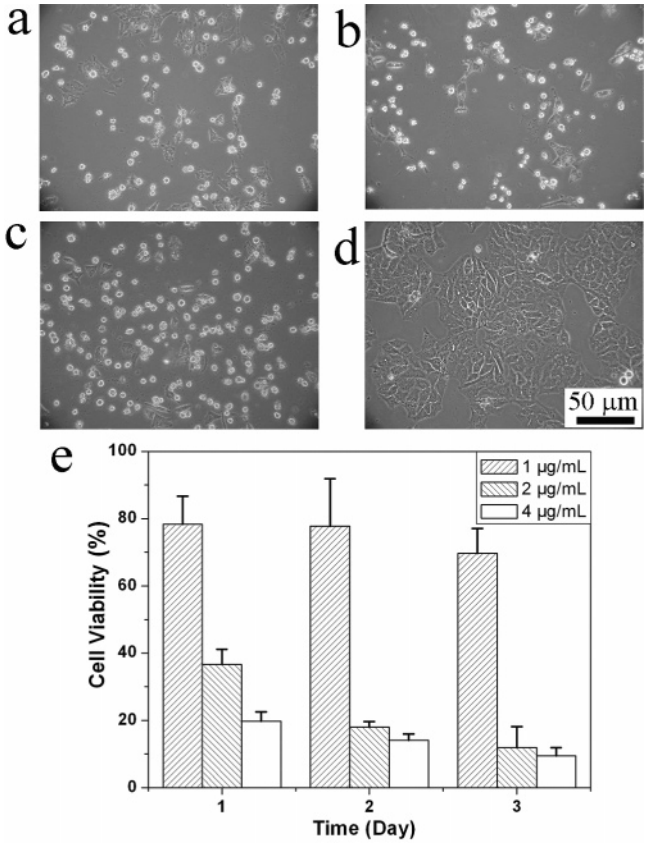

Figure 2. Cytotoxicity analyses of FePt@CoS_2 yolk−shell nanocrystals on HeLa cells. Optical microscopy images of HeLa cells incubated for (a) 24, (b) 48, and (c) 72 h with 5 μg/mL of FePt@CoS_2 nanocrystals and (d) for 48 h with only the growth medium as the negative control (the scale bars presented in panel d is the same for panels a−c). (e) Results of MTT assay of FePt@CoS_2 yolk−shell nanocrystals on HeLa cells at 1.0, 2.0, and 4.0 μg/mL, respectively.

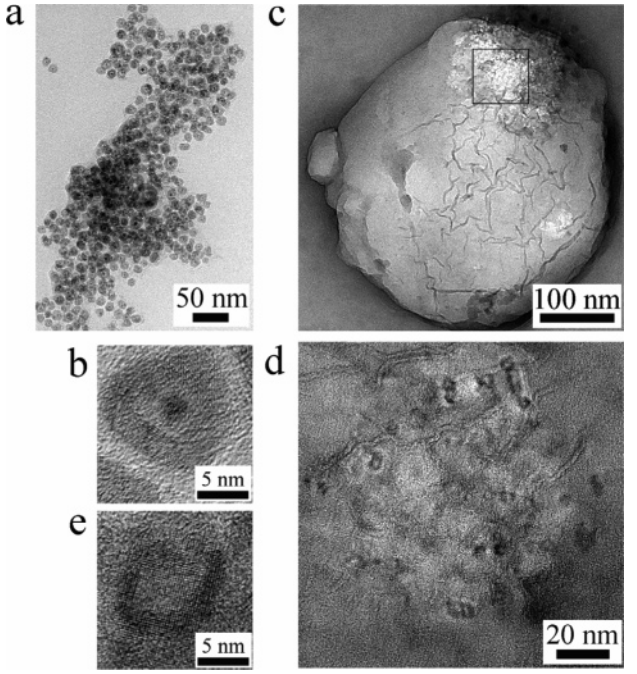

Figure 3. Transformation of FePt@CoS_2 yolk−shell nanocrystals before and after incubation with HeLa cells. (a) TEM and (b) HRTEM images of FePt@CoS_2 yolk−shell nanocrystals dispersed in deionized water for more than 3 days but not incubated with HeLa cells. (c) Representative TEM image of mitochondria from HeLa cells incubated with 4.0 μg/mL of FePt@CoS_2 yolk−shell nanocrystals for 3 days. (d) Magnification of the TEM image in panel c. (e) HRTEM image of FePt@CoS_2 yolk−shell nanocrystals in mitochondria of HeLa cells: a few hollow CoS_2 nanocrystals without FePt cores are randomly dispersed in the organelles (mitochondria).

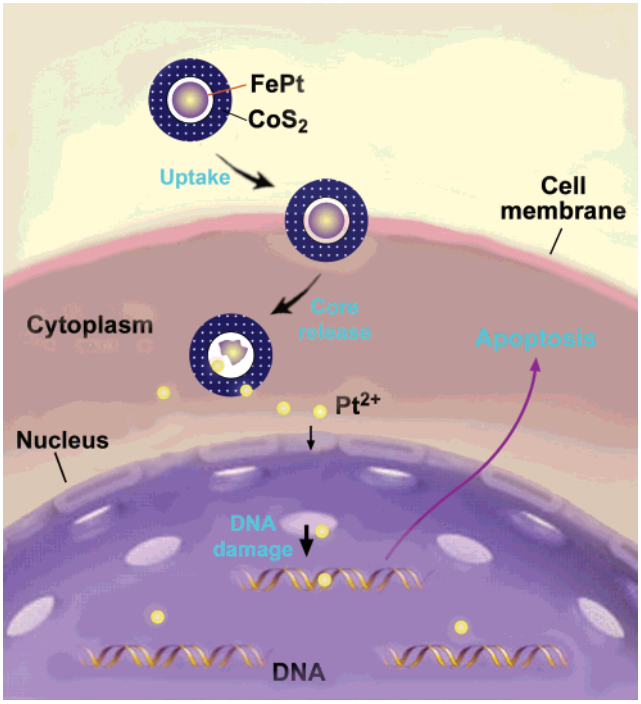

Figure 4. Illustration of a possible mechanism accounting for FePt@CoS_2 yolk−shell nanocrystals killing HeLa cells. After cellular uptake, FePt nanoparticles were oxidized to give Fe^{3+} (omitted for clarity) and Pt^{2+} ions (yellow). The Pt^{2+} ions enter into the nucleus (and mitochondria), bind to DNA, and lead to apoptosis of the HeLa cell.

spectroscopic (XRF) analysis indicates that the ratio of Co and S is 1:2, and it also shows that the ratio of FePt and CoS_2 is about 1:65 (Figure S3). Magnetization measurement also confirms the superparamagnetic character of the FePt@CoS_2 yolk−shell nanocrystals: standard zero-field cooling (ZFC) and field cooling (FC) measurements (Figure S3) give an estimated blocking temperature of ~14 K for the FePt@CoS_2 yolk−shell nanocrystals, which have a coercivity (H_c) of ~350 Oe with a little hysteretic behavior at 5 K according to the field-dependent magnetization measurement. The well-defined block temperature excludes dipolar interactions between FePt magnetic nanoparticles, which agrees with the yolk−shell nanostructures (i.e., the CoS_2 shells minimize the interactions of the FePt yolks).

After complete removal of their surfactant layers according to the reported procedure,[3] the FePt@CoS_2 yolk−shell nano crystals were no longer able to disperse in hexane but were dispersed very well in water by a brief ultrasonic treatment without any surface modification. This exceptionally good dispersion of FePt@CoS_2 nanocrystals in water proves the hydrophilicity of the CoS_2 surface and facilitates the evaluation of their cytotoxicity. Zeta potential analysis of the nanoparticles proves a negatively charged surface of FePt@CoS_2 nanocrystals, indicating that the surface is sulfide-rich. After being incubated with FePt@CoS_2 nanocrystals (5 μg/mL) for in vitro experiments, the number of dead HeLa cells increased dramatically with the time of incubation (Figure 2a−c), compared to the control experiment (Figure 2d). After 72 h of incubation, almost all of the HeLa cells were dead (Figure 2c), indicating the high

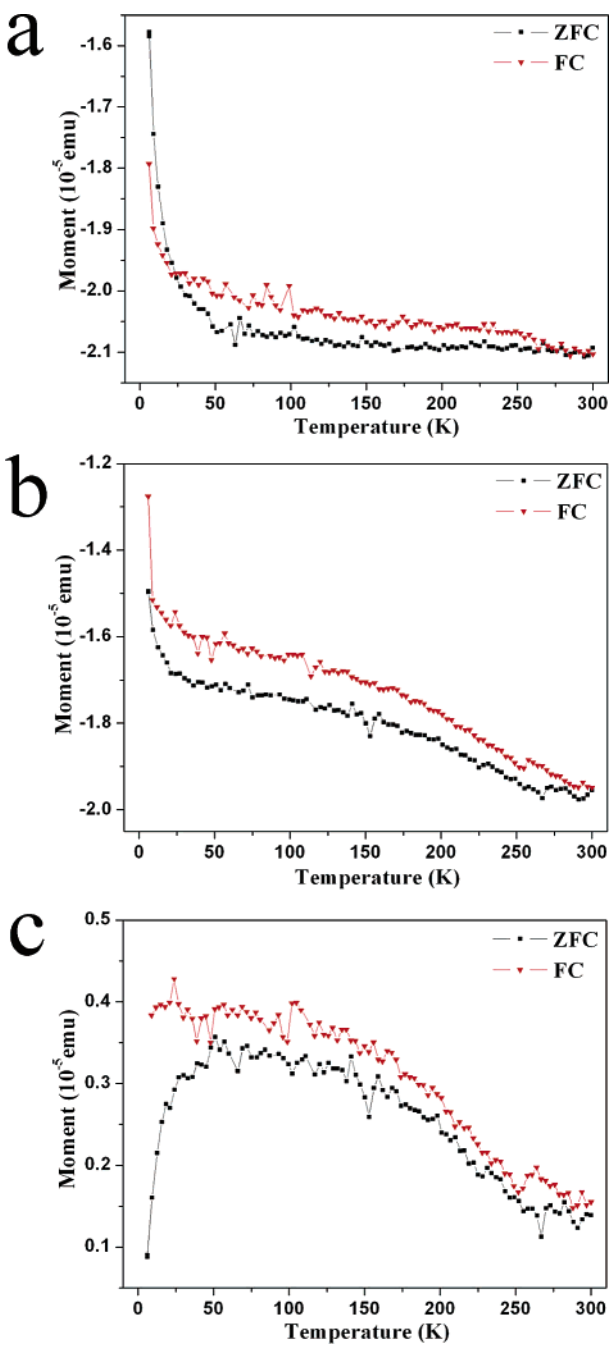

Figure 5. Temperature-dependent magnetization (ZFC/FC) measured with a magnetic field of 200 Oe. Cells suspension before (a) and after (b) incubation with FePt@CoS_2 nanocrystals for 3 days. (c) Difference between the curves shown in panels a and b after two magnetization measurements (extracted by subtracting the signal of control cells from that of FePt@CoS_2 treated cells. The endogenous magnetic species inside the cells may contribute to the systematic difference between FC and ZFC curves.

cytotoxicity of FePt@CoS_2. Upon death, HeLa cells detached from the surface and sprouted multiple small, white buds around the surface of the cells (Figure S4), suggesting the apoptosis of the HeLa cells.[8] Evaluation by MTT assay over a range of doses of FePt@CoS_2 nanocrystals (Figure 2e) indicates their IC_{50} at about 1.5 ± 0.2 μg/mL, which corresponds to about 35.5 ± 4.7 ng of Pt/mL according to the composition of FePt@CoS_2 nanocrystals. This value is much lower than the recorded IC_{50} for cisplatin (230 ng of Pt/mL) in terms of the amount of platinum.[7] The slow dissolution of FePt cores likely increases the cytotoxicity of the york-shell nanoparticles, which agrees with the continuing cell death over time (Figure 2e). Because few anticancer drugs have shown IC_{50} values lower than that of cisplatin in terms of the amount of platinum, this result suggests that FePt@CoS_2 may serve as a useful lead for developing anticancer nanomedicine. Moreover, the minimum inhibitory concentration (MIC) value of FePt@CoS_2 nanocrystals against *Bacillus subtilis* (ATCC 11774) is about 10 μg/mL, suggesting that FePt@CoS_2 nanocrystals also have antibacterial ability (Figure S5).

We used TEM to examine the transformation of the FePt@CoS_2 nanocrystals after they were incubated with HeLa cells. As shown in Figure 3, the FePt@CoS_2 yolk−shell nanocrystals dispersed well in deionized water and showed no structure evolution after more than 3 days (Figure 3a,b). After being incubated with HeLa cells for 3 days at 37 °C and 5% CO_2, many nanocrystals were observed by TEM in organelles such as mitochondria from the HeLa cells (Figure 3c,d), indicating the cellular uptake of FePt@CoS_2 yolk−shell nano crystals. One interesting observation from the TEM image is that there are no more FePt@CoS_2 yolk−shell nanocrystals (Figure 3d) except for some hollow nanospheres (or destroyed hollow nanostructures) in mitochondria bodies, suggesting that the FePt@CoS_2 yolk−shell nanocrystals lose the FePt yolks and can enter into organelles after cellular uptake. The HRTEM image further confirms that the size of hollow nanospheres (Figure 3e) in the cells is similar to the size of CoS_2 shell of the FePt@CoS_2 yolk−shell nanocrystals (Figure 3b). The CoS_2 hollow nanospheres still remain crystalline after cellular uptake. On the basis of the TEM results and the endocytosis-like pathways,[9] we suggest the following plausible process of transformation of FePt@CoS_2 nanocrystals when they incubated with HeLa cells: Being surrounded by cytoplasmic extensions, the FePt@CoS_2 nanocrystals are easily engulfed in the cell to form a vesicle, known as a phagosome. The phagosome could be recognized by one or more primary lysosomes which fuse with the phagosome to form a secondary lysosome. In the secondary lysosome, with a low-pH (pH < 5.5) environment,[10] FePt cores are easily oxidized and destroyed because of the reactivity of uncoated FePt nanoparticles. When digestion is complete, the lysosomal membrane may rupture and discharge its contents (including hollow CoS_2 nanospheres and platinum and iron ions) into the cytoplasm. The hollow CoS_2 nanospheres may then attach onto or enter into organelles, and Pt^{2+} ions also can easily enter into organelles such as nucleus and mitochondria. In order to simulate the process of digestion of FePt@CoS_2 nanocrystals in HeLa cells, we incubated FePt@CoS_2 nanocrystals with phosphate-buffered saline (pH = 4.98) under the same conditions (i.e., 37 °C and 5% CO_2). The FePt core parts were easily destroyed under these simulation conditions and dissolved over time. After 3 days, although a few CoS_2 shells are partially destroyed because of the acidic environment, the FePt parts have almost completely disappeared according the TEM images and EDX analysis (Figure S6). The simulation experiments support the endocytosis and digestion process of

(8) Zhang, W. H.; Tsan, R.; Schroit, A. J.; Fidler, I. J. *Cancer Res.* **2005**, *65*, 11529.
(9) Mellman, I. *Annu. Rev. Cell Dev. Biol.* **1996**, *12*, 575.
(10) Demaurex, N. *News Physiol. Sci.* **2002**, *17*, 1.

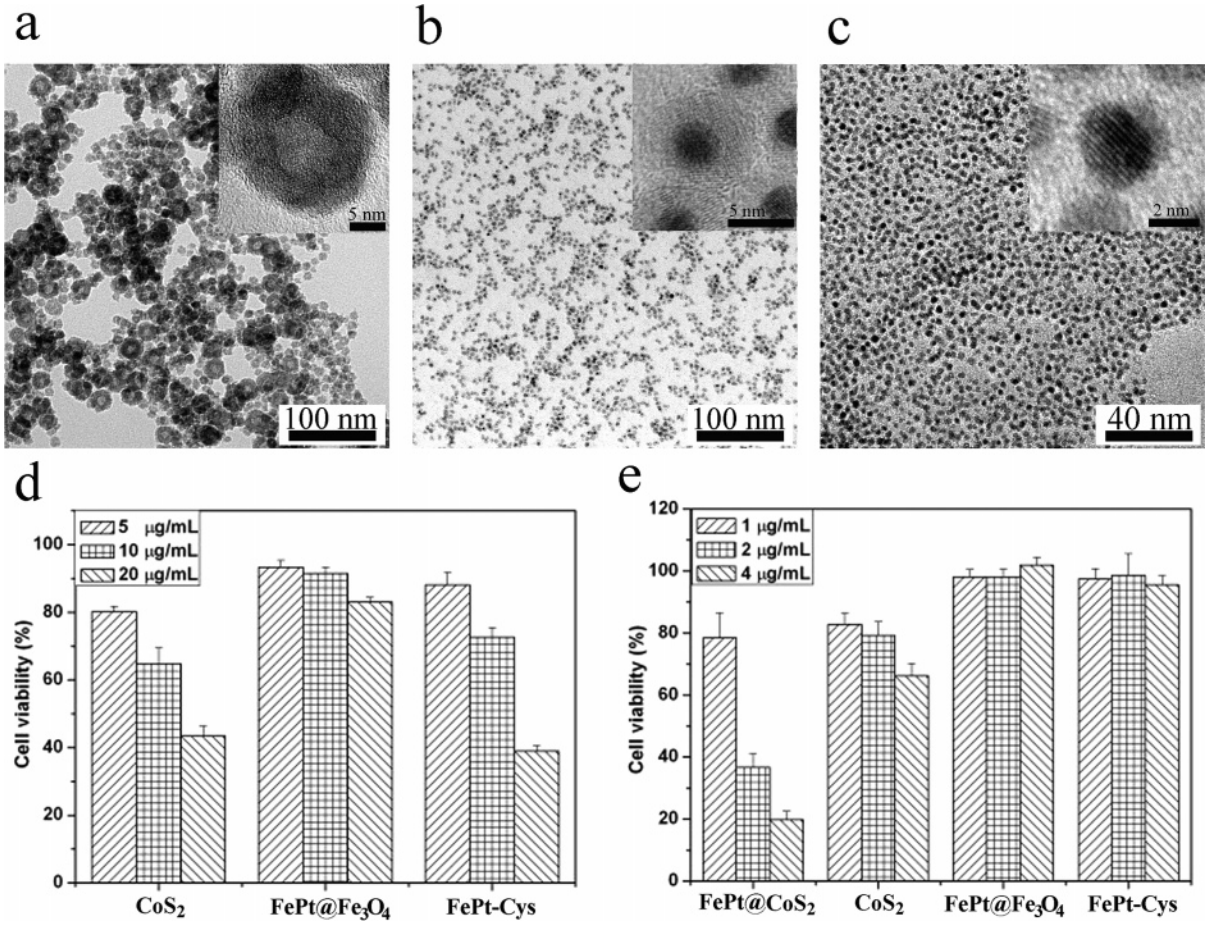

Figure 6. TEM images and cytotoxicity analyses of three control samples. TEM images of (a) CoS_2 hollow nanospheres, (b) FePt@Fe_3O_4 core−shell nanoparticles, and (c) cysteine-coated FePt nanoparticles (inset: HRTEM images). (d) Results of MTT assay for 24 h of CoS_2 hollow nanospheres, FePt@Fe_3O_4 core−shell nanoparticles, and cysteine-coated FePt nanoparticles on HeLa cells at 5.0, 10.0, and 20.0 μg/mL, respectively. (e) Results of MTT assay for 24 h of FePt@CoS_2 yolk−shell nanocrystals, CoS_2 hollow nanospheres, FePt@Fe_3O_4 core−shell nanoparticles, and FePt-Cys nanoparticles on HeLa cells at 1.0, 2.0, and 4.0 μg/mL, respectively, indicating that CoS_2 hollow nanospheres, FePt@Fe_3O_4 core−shell nanoparticles, and FePt-Cys nanoparticles have much lower cytotoxicity than FePt@CoS_2 yolk−shell nanocrystals.

FePt@CoS_2 yolk−shell nanocrystals in HeLa cells. Moreover, the slow dissolution of the FePt parts clearly correlates with the increased toxicity with increasing time of incubation, indicated by the MTT assay (Figure 2e).

Therefore, we propose the mechanism of cytotoxicity of FePt@CoS_2 yolk−shell nanocrystals against the HeLa cells as shown in Figure 4: The nanosized FePt particles (~2 nm in diameter) have no surface protection group after the formation of CoS_2 shells via the Kirkendall effect, and thus they are highly reactive. After cellular uptake, under the acidic environment inside the secondary lysosomes, FePt cores are oxidized and destroyed to become metal ions because the reactivity of unprotected iron promotes the disintegration of FePt to release platinum ions (Pt^{2+}). The permeability (or the rupture) of CoS_2 shells allows these Pt^{2+} ions to diffuse out of the shells easily and enter into the nucleus and mitochondria, damage the DNA double-helix chains by coordinating with 5′-GG-3′ bases of DNA,[11] and lead to the apoptosis of the HeLa cells.

To further verify the mechanism proposed in Figure 4, we measured temperature-dependent magnetization (ZFC/FC) of cells before and after they were incubated (3 days at 37 °C and 5% CO_2) with FePt@CoS_2 yolk−shell nanocrystals. The magnetization curves in Figure 5a indicate that the cells, before being incubated with FePt@CoS_2 nanocrystals, are mainly diamagnetic, as we expected for the organic compounds and the cells. The strong increase in magnetization in the low-temperature region should be due to the paramagnetic species in cells (e.g., metal centers of metalloenzymes). After the cells were incubated with FePt@CoS_2 nanocrystals for 3 days, the magnetization curves for the cells (Figure 5b) were certainly different from those of the control sample (Figure 5a) and those of the FePt@CoS_2 nanocrystals (Figure S3). In addition to the contribution of the paramagnetic ions that inherently associate with the cells, there is another positive signal in the temperature range 6−250 K (Figure 5c, extracted by subtracting the signal of the control cells from that of FePt@CoS_2-treated cells). The broad peak between 6 and 250 K likely arises from magnetic clusters of iron oxides or iron hydroxides with a broad size distribution because of the reaction of iron ions with water after the degradation of the FePt core. Together with the TEM results, these magnetic data also indirectly support the mechanism illustrated in Figure 4.

To prove that the observed ultrahigh cytotoxicity of the FePt@CoS_2 yolk−shell nanocrystals mainly arises from the uncoated FePt core, we performed a series of control experi-

(11) Yang, D.; van Boom, S. S.; Reedijk, J.; van Boom, J. H.; Wang, A. H. *Biochemistry* **1995**, *34*, 12912. Takahara, P. M.; Rosenzweig, A. C.; Frederick, C. A.; Lippard, S. J. *Nature* **1995**, *377*, 649. Takahara, P. M.; Frederick, C. A.; Lippard, S. J. *J. Am. Chem. Soc.* **1996**, *118*, 12309.

ments by incubating HeLa cells with CoS_2 hollow nanospheres (Figure 6a), FePt@Fe_3O_4 core−shell nanoparticles (Figure 6b), and cysteine-coated FePt nanoparticles (Figure 6c). CoS_2 hollow nanospheres were synthesized as in the previous procedure[3] but without FePt nanoparticles. FePt@Fe_3O_4 core−shell nanoparticles were synthesized as described in a previous publication.[12] According to the cytotoxicity assay shown in Figure 6, CoS_2 hollow nanocrystals have a low cytotoxicity and exhibit an IC_{50} of 13.8 ± 1.8 μg/mL (Figure 6d). FePt@Fe_3O_4 core−shell nanoparticles show very little cytotoxicity (Figure 6d), suggesting that FePt nanoparticles inside the Fe_3O_4 shells are very stable and resistant to oxidization because of the biocompatible, compact Fe_3O_4 shells. Because the organic protection layer retards the oxidation of FePt nanoparticles, cysteine-coated FePt nanoparticles also show very low cytotoxicity and exhibit an IC_{50} of 15.5 ± 1.2 μg/mL (Figure 6d), corresponding to 12.0 ± 0.9 μg of Pt/mL. Compared with FePt@CoS_2 yolk−shell nanocrystals, the three control samples, CoS_2 hollow nanospheres, FePt@Fe_3O_4 core−shell nanoparticles, and FePt-Cys nanoparticles, have lower cytotoxicity (Figure 6e), which supports the mechanism illustrated in Figure 4. The results of MTT assays using CoS_2 hollow nanospheres and FePt-Cys nanoparticles for 3 days showed that the cells recover dramatically after day two (Figure S7), indicating that these two compounds only possess acute toxicity.

(12) Chen, M.; Liu, J. P.; Sun, S. H. *J. Am. Chem. Soc.* **2004**, *126*, 8394.

Conclusion

In summary, we have synthesized a new yolk−shell nanostructure, FePt@CoS_2 yolk−shell nanocrystals, and evaluated its cytotoxicity. Although the ultrahigh cytotoxicity originating in the uncoated FePt yolk in the FePt@CoS_2 nanocrystals would also be associated with side effects (similar to cisplatin), this type of yolk−shell or core−shell nanostructures may lead to novel nanomedicines for treating cancers, resulting from decorating the surface of the FePt@CoS_2 nanocrystals with cancer-targeting antibodies.

Acknowledgment. This work was partially supported by RGC, HIA (HKUST), and the DuPont Co.

Supporting Information Available: Experimental section and Figures S1−S7. This material is available free of charge via the Internet at http://pubs.acs.org.

JA067785E